

# Radiative Scalar Meson Decays in the Light-Front Quark Model

Martin A. DeWitt<sup>a</sup>, Ho-Meoyng Choi<sup>b</sup> and Chueng-Ryong Ji<sup>a</sup>

<sup>a</sup> Department of Physics, North Carolina State University, Raleigh, NC 27695-8202

<sup>b</sup> Department of Physics, Kyungpook National University, Daegu, 702-701 Korea

We construct a relativistic  ${}^3P_0$  wavefunction for scalar mesons within the framework of light-front quark model(LFQM). This scalar wavefunction is used to perform relativistic calculations of absolute widths for the radiative decay processes  $(0^{++}) \rightarrow \gamma\gamma$ ,  $(0^{++}) \rightarrow \phi\gamma$ , and  $(0^{++}) \rightarrow \rho\gamma$  which incorporate the effects of glueball- $q\bar{q}$  mixing. The mixed physical states are assumed to be  $f_0(1370)$ ,  $f_0(1500)$ , and  $f_0(1710)$  for which the flavor-glue content is taken from the mixing calculations of other works. Since experimental data for these processes are poor, our results are compared with those of a recent non-relativistic model calculation. We find that while the relativistic corrections introduced by the LFQM reduce the magnitudes of the decay widths by 50-70%, the relative strengths between different decay processes are fairly well preserved. We also calculate decay widths for the processes  $\phi \rightarrow (0^{++})\gamma$  and  $(0^{++}) \rightarrow \gamma\gamma$  involving the light scalars  $f_0(980)$  and  $a_0(980)$  to test the simple  $q\bar{q}$  model of these mesons. Our results of  $q\bar{q}$  model for these processes are not quite consistent with well-established data, further supporting the idea that  $f_0(980)$  and  $a_0(980)$  are not conventional  $q\bar{q}$  states.

## I. INTRODUCTION

As is well known, the assignment of the scalar ( $J^{PC} = 0^{++}$ )  $q\bar{q}$  states has long been an enigma in hadron spectroscopy. Unlike the elegant, ideally mixed vector and tensor multiplets, it is still controversial which are the members of the expected  $L = S = 1$   $q\bar{q}$  multiplet since there are now too many  $0^{++}$  mesons observed in the region below 2 GeV for them all to be explained naturally within a  $q\bar{q}$  picture[1]. For example, 2 isovector ( $IJ^{PC} = 1\ 0^{++}$ ) [ $a_0(980)$ ,  $a_0(1450)$ ] and 5 isoscalar ( $0\ 0^{++}$ ) [ $f_0(600)$ (or  $\sigma$ ),  $f_0(980)$ ,  $f_0(1370)$ ,  $f_0(1500)$ ,  $f_0(1710)$ ] states have been reported by the Particle Data Group[1]. This has led to the suggestion that not all of them are  $q\bar{q}$  states. The main reason for this situation is that around the relevant mass region there exist other kinds of particles such as  $K\bar{K}$  molecules[2, 3, 4], glueballs[5, 6], four-quark ( $qq\bar{q}\bar{q}$ ) systems[7], or hybrids.

Interpreting the structure of each of the known scalars has proven to be a fairly controversial endeavor. Take, for example, the light scalars (*i.e.* those below 1 GeV). Due to some of the difficulties associated with  $f_0(980)$  and  $a_0(980)$ —*e.g.* the strong couplings to  $K\bar{K}$  in spite of their masses being at the  $K\bar{K}$  threshold, and the large discrepancies of  $\pi\pi$ [3],  $\gamma\gamma$ [4] and  $\phi$ -radiative decay[8] widths between non-relativistic (NR) quark model predictions and experimental data—Weinstein and Isgur[2] proposed the isospin  $I = 0$   $f_0(980)$  and the  $I = 1$   $a_0(980)$  within the NR potential model as the “ $K\bar{K}$  molecules”. However, a more conventional interpretation for these states has been given by Törnqvist and Roos[9] who analyzed the data on the  $f_0(980)$ ,  $f_0(1370)$ ,  $a_0(980)$  and  $a_0(1450)$  as unitarized remnants of  $q\bar{q}$   ${}^3P_0$  states with six parameters and theoretical constraints including flavor symmetry, the OZI rule, the equal-spacing rule for the bare  $q\bar{q}$  states, unitarity, and analyticity. In this work, the authors concluded that the  $f_0(980)$  and the  $f_0(1370)$  are two manifestations of the same  $s\bar{s}$ , while the  $a_0(980)$

and the  $a_0(1450)$  are two manifestations of the same  $u\bar{d}$  state.

The interpretation of the structures of some of the heavier scalars has been somewhat less controversial. For example,  $f_0(1370)$  and  $a_0(1450)$  are most commonly interpreted as  $q\bar{q}$  states, even though the flavor assignments for each are still unclear. Also, there appears to be general agreement on identifying  $f_0(1500)$  as a glueball, possibly mixed with  $n\bar{n} = (u\bar{u} + d\bar{d})/\sqrt{2}$  and  $s\bar{s}$ . This interpretation has followed both from lattice QCD which, in the quenched approximation, predicts that the lightest glueball has  $J^{PC} = 0^{++}$  and a mass of 1.55–1.74 GeV [10, 11], as well as from the fact that  $f_0(1500)$  decays strongly into  $\pi\pi$  but not into  $K\bar{K}$ .

Most recently, Close and Törnqvist[12] have proposed a scheme which sorts the light scalars into two distinct nonets: one nonet above 1 GeV and another below 1 GeV, with different physics operating in each. The nonet above the 1 GeV threshold is comprised of the  $q\bar{q}$  states mixed with the scalar glueball. The glueball’s presence is inferred from the overpopulation of isoscalars in this mass region. The nonet below 1 GeV is made up of  $qq\bar{q}\bar{q}$  and meson-meson molecules. As such,  $f_0(980)$  and  $a_0(980)$  can be thought of as superpositions of four-quark states and  $K\bar{K}$  molecules. The authors of Ref. [12] demonstrate that such a scheme involving two scalar nonets can be described using two coupled linear sigma models.

In this paper, we investigate various radiative scalar meson decays which could provide important clues on the internal structures of these states[8, 13]. For the calculations, we employ the light-front quark model (LFQM) which has been used very successfully in the past to compute decay rates for pseudoscalar, vector, and axial-vector mesons [14, 15, 16]. Extending the model to include scalar states mainly involves the construction of a new  ${}^3P_0$  light-front model wavefunction. In section II, we give the detailed form of this wavefunction and explain how the model parameters are obtained. This new

scalar wavefunction is used to study the radiative decays of the heavy scalars  $f_0(1370)$ ,  $f_0(1500)$ , and  $f_0(1710)$ , as well as the light scalars  $a_0(980)$  and  $f_0(980)$ .

In the case of the heavy scalars, we adopt the scheme of Close and Törnqvist in which  $f_0(1370)$ ,  $f_0(1500)$ , and  $f_0(1710)$  are considered to be mixtures of  $n\bar{n}$ ,  $s\bar{s}$ , and  $gg$ . The flavor–glue content of each state is taken from mixing analyses done by Lee and Weingarten [17] and by Close and Kirk [18]. Taken together, these works provide mixing amplitudes for three distinct cases of the scalar glueball mass: (1) a heavy glueball ( $M_{n\bar{n}} < M_{s\bar{s}} < M_{gg}$ ), (2) a medium weight glueball ( $M_{n\bar{n}} \lesssim M_{gg} < M_{s\bar{s}}$ ), and (3) a light glueball ( $M_{gg} < M_{n\bar{n}} < M_{s\bar{s}}$ ). The details of these three mixing scenarios are outlined in section III. In the case of the light scalars,  $a_0(980)$  and  $f_0(980)$  are assumed to be conventional  $q\bar{q}$  states. The flavor content of  $a_0(980)$  is then  $(u\bar{u} - d\bar{d})/\sqrt{2}$ , and that of  $f_0(980)$  is some superposition of  $n\bar{n}$  and  $s\bar{s}$ . Rather than attempting to determine the degree of mixing for  $f_0(980)$ , it suffices to examine the two ideally mixed cases:  $f_0(980) = n\bar{n}$  and  $f_0(980) = s\bar{s}$ .

In section IV, the general forms of the  $Q^2$ -dependent transition form factors for the processes  $(1^{--}) \rightarrow (0^{++})\gamma^*$ ,  $(0^{++}) \rightarrow (1^{--})\gamma^*$ , and  $(0^{++}) \rightarrow \gamma\gamma^*$  are derived. In the limit as  $Q^2 \rightarrow 0$ , these form factors yield the decay constants for the real photon processes which can then be used to compute the corresponding decay widths. In section V–A, we present our numerical results for the heavy scalars. This includes the form factors and decay widths for the specific processes  $f_0 \rightarrow \phi\gamma$ ,  $f_0 \rightarrow \rho\gamma$ , and  $f_0 \rightarrow \gamma\gamma$ . Our results for the light scalars involved in the processes  $\phi \rightarrow f_0(a_0)\gamma$  and  $f_0(a_0) \rightarrow \gamma\gamma$  are given in section V–B. A summary of the paper’s salient points and a brief discussion of our intended future work is given in section VI. In the Appendix, the explicit form of the trace used in section IV.A is presented.

## II. THE MODEL WAVEFUNCTIONS

One of the popular quark models in the light-front formalism is the invariant meson mass(IM) scheme[19, 20] in which the invariant meson mass square  $M_0^2$  is given by

$$M_0^2 = \sum_i^2 \frac{\mathbf{k}_{i\perp}^2 + m_i^2}{x_i}. \quad (1)$$

In our analysis, we will only consider the light-meson sector( $u, d$ , and  $s$  quarks) with equal quark and anti-quark masses( $m_q = m_{\bar{q}}$ ).

The light-front  $q\bar{q}$  bound-state wavefunction of the scalar( ${}^3P_0$ ) and vector( ${}^3S_1$ ) mesons can be written in the following covariant form

$$\begin{aligned} \Psi_M(x_i, \mathbf{k}_{i\perp}, \lambda_i) &= \bar{u}_{\lambda_q}(p_q)\Gamma_M v_{\lambda_{\bar{q}}}(p_{\bar{q}})\phi_M(x_i, \mathbf{k}_{i\perp}) \\ &= \mathcal{R}_{\lambda_q\lambda_{\bar{q}}}^M(x_i, \mathbf{k}_{i\perp})\phi_M(x_i, \mathbf{k}_{i\perp}), \end{aligned} \quad (2)$$

where  $\mathcal{R}_{\lambda_q\lambda_{\bar{q}}}^M$  is the spin-orbit wavefunction, which is obtained by the interaction independent Melosh transfor-

mation from the ordinary equal-time static spin-orbit wavefunction, and  $\phi_M(x_i, \mathbf{k}_{i\perp})$  is the radial wavefunction. The operators  $\Gamma_M$  for the scalar(S) and vector(V) mesons are given by

$$\begin{aligned} \Gamma_S &= \frac{(\not{P}_S + M_0^S)\left(\frac{K \cdot \not{P}_S}{M_0^S} - \not{K}\right)}{(M_0^S + m_q + m_{\bar{q}})\sqrt{2[(M_0^S)^2 - (m_q^2 - m_{\bar{q}}^2)]}} \\ \Gamma_V &= \frac{-(\not{P}_V + M_0^V)\not{\epsilon}(J_3)}{(M_0^V + m_q + m_{\bar{q}})\sqrt{2[(M_0^V)^2 - (m_q^2 - m_{\bar{q}}^2)]}}, \end{aligned} \quad (3)$$

where  $P_{(S,V)} \equiv (p_q + p_{\bar{q}})$ ,  $K \equiv (p_{\bar{q}} - p_q)/2$  is the relative four-momentum between the quark and antiquark, and  $\epsilon$  is the polarization four-vector of the vector meson(with momentum  $P_V$ ), which is given by

$$\begin{aligned} \epsilon^\mu(\pm) &= [\epsilon^+, \epsilon^-, \epsilon_\perp] = \left[0, \frac{2}{P_V^+}\epsilon_\perp(\pm) \cdot \mathbf{P}_{V\perp}, \epsilon_\perp(\pm)\right], \\ \epsilon_\perp(\pm) &= \mp \frac{(1, \pm i)}{\sqrt{2}}, \\ \epsilon^\mu(0) &= \frac{1}{M_V} \left[P_V^+, \frac{\mathbf{P}_{V\perp}^2 - M_V^2}{P_V^+}, \mathbf{P}_{V\perp}\right]. \end{aligned} \quad (4)$$

The operator  $\Gamma_V$  was derived in Ref. [21]. We followed the same procedure, detailed in Ref. [21], in order to derive  $\Gamma_S$ . Note that in the case of the vector meson, the operator  $\Gamma_V$  has the expected form,  $(\not{P} + M)\not{\epsilon}$ . However, because the scalar ( ${}^3P_0$ ) state possesses non-zero orbital angular momentum, the proper Melosh-transformed spin-orbit wavefunction is not simply given by  $\Gamma_S = (\not{P} + M)$ , as one might expect. The form is more complicated as shown in Eq.(3), and it depends explicitly upon the relative momentum between the meson’s constituents. This same type of behavior was demonstrated for the axial–vector meson in Ref. [21]. Since the axial–vector ( ${}^3P_1$ ) state also possesses non-zero orbital angular momentum, the spin-orbit wavefunction is not simply given by  $(\not{P} + M)\not{\epsilon}\gamma^5$ . The correct form contains an additional factor which explicitly depends on the relative momentum between the quark and anti-quark. It is interesting to note, however, that in the case where  $m_q = m_{\bar{q}} = m$  (which we use throughout this work), the expressions in Eq. (3) reduce to

$$\begin{aligned} \Gamma_S &= \frac{1}{2\sqrt{2}M_0^S}(\not{P}_S + M_0^S), \\ \Gamma_V &= \frac{-1}{\sqrt{2}M_0^V(M_0^V + 2m)}(\not{P}_V + M_0^V)\not{\epsilon}(J_3). \end{aligned} \quad (5)$$

So, in the equal mass case,  $\Gamma_S$  does have the expected form. We confirmed the similar reduction of the axial–vector meson wavefunction in the equal mass case. These expressions can be further simplified to the form we will

use in our analysis:

$$\begin{aligned}\Gamma_S &= \frac{1}{2\sqrt{2}}, \\ \Gamma_V &= \frac{-1}{\sqrt{2}M_0^V} \left[ \not{\epsilon}(J_3) - \frac{\epsilon \cdot (p_q - p_{\bar{q}})}{M_0^V + 2m} \right].\end{aligned}\quad (6)$$

The spin-orbit wavefunctions satisfy the following relations

$$\begin{aligned}\sum_{\lambda_q \lambda_{\bar{q}}} \mathcal{R}_{\lambda_q \lambda_{\bar{q}}}^{S\dagger} \mathcal{R}_{\lambda_q \lambda_{\bar{q}}}^S &= \frac{1}{4}(M_0^2 - 4m^2) = |\mathbf{k}|^2, \\ \sum_{\lambda_q \lambda_{\bar{q}}} \mathcal{R}_{\lambda_q \lambda_{\bar{q}}}^{V\dagger} \mathcal{R}_{\lambda_q \lambda_{\bar{q}}}^V &= 1,\end{aligned}\quad (7)$$

where  $\mathbf{k} = (\mathbf{k}_\perp, k_z)$  is the three momentum of the constituent quark and  $k_z = (x - \frac{1}{2})M_0$ . Note that the total wavefunction  $\Psi_S(x, \mathbf{k}_\perp)$  for the scalar meson vanishes at  $|\mathbf{k}| = 0$  in accordance with the property of  $P$ -wave function.

For the radial wavefunctions  $\phi_M(x_i, \mathbf{k}_{i\perp})$ , we shall use the following gaussian wavefunctions for the scalar and vector mesons

$$\begin{aligned}\phi_S(x, \mathbf{k}_\perp) &= \mathcal{N} \sqrt{\frac{2}{3\beta^2}} \sqrt{\frac{\partial k_z}{\partial x}} \exp(-\mathbf{k}^2/2\beta^2), \\ \phi_V(x, \mathbf{k}_\perp) &= \mathcal{N} \sqrt{\frac{\partial k_z}{\partial x}} \exp(-\mathbf{k}^2/2\beta^2),\end{aligned}\quad (8)$$

where  $\mathcal{N} = 4(\frac{\pi}{\beta^2})^{3/4}$  and  $\partial k_z/\partial x$  is the Jacobian of the variable transformation  $\{x, \mathbf{k}_\perp\} \rightarrow \mathbf{k} = (k_z, \mathbf{k}_\perp)$  defined by

$$\frac{\partial k_z}{\partial x} = \frac{M_0}{4x(1-x)},\quad (9)$$

and the normalization factors are obtained from the following normalization of the total wavefunction,

$$\int_0^1 dx \int \frac{d^2 \mathbf{k}_\perp}{16\pi^3} |\Psi_M(x_i, \mathbf{k}_\perp)|^2 = 1.\quad (10)$$

The wavefunctions depend on only two model parameters: the constituent quark mass,  $m$ , and the binding strength,  $\beta$ . For these parameters, we use the values determined in Ref. [14] which are ( $m_{u,d} \equiv m_n = 0.22$  GeV,  $\beta_{u,d} \equiv \beta_n = 0.3659$  GeV) and ( $m_s = 0.45$  GeV,  $\beta_s = 0.4128$  GeV). These values were obtained by fitting the LFQM spectrum for pseudoscalar and vector mesons—obtained using a QCD-inspired model Hamiltonian with a linear confining potential—to experimental data. In this paper, we will use these values of the parameters for both vector and scalar mesons. In a future work, we intend to perform a separate fit to scalar meson data to see whether or not the model parameters would differ significantly.

Since our analysis deals with  $\phi$  decays, a value for the  $\omega$ - $\phi$  mixing angle is necessary. We use  $\delta_{\omega-\phi} = \pm 7.8^\circ$

(the sign cannot be fixed), which was also determined in Ref. [14]. This value was obtained by a mass squared mixing analysis in which it was assumed that

$$\begin{aligned}|\phi\rangle &= -\sin \delta_{\omega-\phi} |n\bar{n}\rangle - \cos \delta_{\omega-\phi} |s\bar{s}\rangle \\ |\omega\rangle &= \cos \delta_{\omega-\phi} |n\bar{n}\rangle - \sin \delta_{\omega-\phi} |s\bar{s}\rangle,\end{aligned}$$

and in which the masses of the bare quarkonia were determined using the model parameters and Hamiltonian mentioned in the previous paragraph.

### III. SCALAR MIXING AMPLITUDES

Glueball- $q\bar{q}$  mixing can be described using a mass mixing matrix. Written in the  $|gg\rangle, |s\bar{s}\rangle, |n\bar{n}\rangle$  basis, this takes the form [17, 18]

$$M = \begin{pmatrix} M_{gg} & f & \sqrt{2}fr \\ f & M_{s\bar{s}} & 0 \\ \sqrt{2}fr & 0 & M_{n\bar{n}} \end{pmatrix},\quad (11)$$

where  $f = \langle gg|M|s\bar{s}\rangle$  and  $r = \langle gg|M|n\bar{n}\rangle/\sqrt{2}\langle gg|M|s\bar{s}\rangle$ . As described in the introduction, the mixing is assumed to be among the three isoscalar states  $f_0(1370)$ ,  $f_0(1500)$  and  $f_0(1710)$ . These mixed physical states can be written as

$$\begin{pmatrix} |f_0(1710)\rangle \\ |f_0(1500)\rangle \\ |f_0(1370)\rangle \end{pmatrix} = \begin{pmatrix} a_1 & b_1 & c_1 \\ a_2 & b_2 & c_2 \\ a_3 & b_3 & c_3 \end{pmatrix} \begin{pmatrix} |gg\rangle \\ |s\bar{s}\rangle \\ |n\bar{n}\rangle \end{pmatrix},\quad (12)$$

The mixing amplitudes,  $a_i$ ,  $b_i$ , and  $c_i$  can be written in terms of the physical masses ( $M_{f_j}$ ), the bare masses ( $M_{gg}$ ,  $M_{s\bar{s}}$ , and  $M_{n\bar{n}}$ ), and the glueball-bare quarkonia mixing strengths ( $f$  and  $r$ ). For the present analysis we will adopt the values obtained by Lee and Weingarten, and by Close and Kirk.

Beginning with the lattice QCD-motivated assumption that the bare scalar  $s\bar{s}$  is lighter than the scalar glueball (*i.e.*  $M_{n\bar{n}} < M_{s\bar{s}} < M_{gg}$ ), Lee and Weingarten obtained the following mixing amplitudes [17]:

$$\begin{pmatrix} 0.86 \pm 0.05 & 0.30 \pm 0.05 & 0.41 \pm 0.09 \\ -0.13 \pm 0.05 & 0.91 \pm 0.04 & -0.40 \pm 0.11 \\ -0.50 \pm 0.12 & 0.29 \pm 0.09 & 0.82 \pm 0.09 \end{pmatrix}.\quad (13)$$

Using a different approach, Close and Kirk [18] examined the constraints placed on the flavor content of  $f_0(1370)$ ,  $f_0(1500)$ , and  $f_0(1710)$  by decay branching ratios to pairs of pseudoscalar mesons. From a  $\chi^2$  analysis of the available branching ratio data, they obtained various solutions depending on which parameters were left free at the outset. One solution was consistent with a glueball which lies just above the bare  $n\bar{n}$  (*i.e.*  $M_{n\bar{n}} \lesssim M_{gg} < M_{s\bar{s}}$ ). Its associated mixing amplitudes are

$$\begin{pmatrix} 0.39 \pm 0.03 & 0.91 \pm 0.02 & 0.15 \pm 0.02 \\ -0.65 \pm 0.04 & 0.33 \pm 0.04 & -0.70 \pm 0.07 \\ -0.69 \pm 0.07 & 0.15 \pm 0.01 & 0.70 \pm 0.07 \end{pmatrix}.\quad (14)$$

Another of their solutions was consistent with an even lighter glueball which lies below the mass of the  $n\bar{n}$  (*i.e.*  $M_{gg} < M_{n\bar{n}} < M_{s\bar{s}}$ ). The mixing amplitudes for this solution are

$$\begin{pmatrix} 0.25 & 0.96 & 0.10 \\ -0.37 & 0.13 & -0.92 \\ -0.89 & 0.14 & 0.44 \end{pmatrix}. \quad (15)$$

In the next section, we shall obtain expressions for the transition form factors for various radiative decays. Then, in the following section, we will use the mixing amplitudes given in Eqs. (13)–(15) above to numerically evaluate the form factors and corresponding decay widths for the heavy, medium, and light weight glueball cases respectively.

#### IV. FORM FACTORS FOR RADIATIVE DECAYS

##### A. The process $V(S) \rightarrow S(V) + \gamma$

The coupling constant  $g_{AX\gamma}$  for the radiative  $P_A(q_1\bar{q}) \rightarrow P_X(q_2\bar{q})\gamma$  decays between vector (V) and scalar (S) mesons, *i.e.*  $(A, X) = ({}^3S_1, {}^3P_0)$  or  $({}^3P_0, {}^3S_1)$ , is obtained by the matrix element of the electromagnetic current  $J^\mu$  which is defined by

$$\begin{aligned} \mathcal{M}_1 &= \langle X(P_2) | \epsilon_\gamma \cdot J | A(P_1) \rangle \\ &= eg_{AX\gamma} [(\epsilon_\gamma \cdot \epsilon_V)(P_1 \cdot q) - (\epsilon_\gamma \cdot P_1)(\epsilon_V \cdot q)], \end{aligned} \quad (16)$$

where  $\epsilon_\gamma$  and  $\epsilon_V$  are the polarization vectors of the photon and the vector meson, respectively. Since the  $J_z = 0$  state of the vector meson cannot convert into a real photon, the  $\epsilon_V$  should be transversely polarized ( $J_z = \pm 1$ ) to extract the coupling constant  $g_{AX\gamma}$ . In other words, the possible helicity combinations in the transition  $V(S) \rightarrow S(V)\gamma$  are either from  $(J_z^\gamma = +1, J_z^V = -1)$  or from  $(J_z^\gamma = -1, J_z^V = +1)$ . The decay width for  $A \rightarrow X + \gamma$  is given by [22]

$$\Gamma(A \rightarrow X + \gamma) = \alpha \frac{g_{AX\gamma}^2}{2J_A + 1} \left[ \frac{M_A^2 - M_X^2}{2M_A} \right]^3, \quad (17)$$

where  $\alpha$  is the fine structure constant and  $J_A$  is the total angular momentum of the initial particle.

In LFQM calculations, we shall analyze the virtual photon ( $\gamma^*$ ) decay process so that we calculate the momentum dependent transition form factor,  $F_{AX\gamma^*}(Q^2)$ . The coupling constant,  $g_{AX\gamma}$ , can then be determined in the limit as  $Q^2 \rightarrow 0$  (*i.e.*,  $g_{AX\gamma} = F_{AX\gamma^*}(Q^2 = 0)$ ). Figure 1 shows the primary Feynman diagram for this process. The amplitude is

$$\begin{aligned} \mathcal{M}_1^\mu &= \langle X(P_2) | J^\mu | A(P_1) \rangle \\ &= eF_{AX\gamma}(q^2) [\epsilon_V^\mu (P_1 \cdot q) - P_1^\mu (\epsilon_V \cdot q)]. \end{aligned} \quad (18)$$

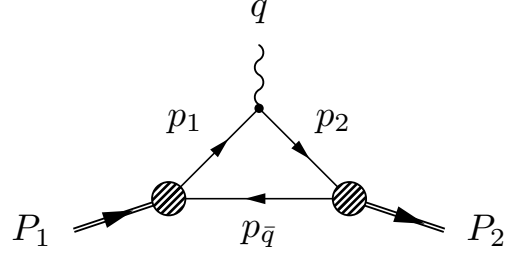


FIG. 1: Primary diagram for  $A(P_1) \rightarrow X(P_2) + \gamma(q)$ . There is an additional diagram in which the virtual photon interacts with the antiquark.

Our analysis is based on the standard light-front frame ( $q^+ = 0$ ) [23].

$$\begin{aligned} P_1 &= (P_1^+, P_1^-, \mathbf{P}_{1\perp}) = (P_1^+, \frac{M_A^2}{P_1^+}, \mathbf{0}_\perp), \\ q &= (0, \frac{M_A^2 - M_X^2 - Q^2}{P_1^+}, \mathbf{q}_\perp), \\ P_2 &= P_1 - q = (P_1^+, \frac{M_X^2 + Q^2}{P_1^+}, -\mathbf{q}_\perp), \end{aligned} \quad (19)$$

where  $\mathbf{q}_\perp^2 = Q^2 = -q^2$  is the space-like photon momentum transfer.

The quark momentum variables in the  $q^+ = 0$  frame are given by

$$\begin{aligned} p_1^+ &= (1-x)P_1^+, \quad p_{\bar{q}}^+ = xP_1^+, \\ \mathbf{p}_{1\perp} &= (1-x)\mathbf{P}_{1\perp} + \mathbf{k}_\perp, \quad \mathbf{p}_{\bar{q}\perp} = x\mathbf{P}_{1\perp} - \mathbf{k}_\perp, \\ p_2^+ &= (1-x)P_2^+, \quad p_{\bar{q}}^{\prime+} = xP_2^+, \\ \mathbf{p}_{2\perp} &= (1-x)\mathbf{P}_{2\perp} + \mathbf{k}'_\perp, \quad \mathbf{p}'_{\bar{q}\perp} = x\mathbf{P}_{2\perp} - \mathbf{k}'_\perp, \end{aligned} \quad (20)$$

which require that  $p_{\bar{q}}^+ = p_{\bar{q}}^{\prime+}$  and  $\mathbf{p}_{\bar{q}\perp} = \mathbf{p}'_{\bar{q}\perp}$ .

The hadronic matrix elements in the radiative decay between two particles  $A$  and  $X$  are of the form

$$\begin{aligned} &\langle X(P_2) | J^\mu | A(P_1) \rangle \\ &= \sum_{j, \lambda_1 \lambda_2} \mathcal{A}_j \int_0^1 dx \int \frac{d^2\mathbf{k}_\perp}{16\pi^3} \phi_2(x, \mathbf{k}'_\perp) \phi_1(x, \mathbf{k}_\perp) \\ &\quad \times \mathcal{R}_{\lambda_2 \lambda_1}^{X^\dagger} \frac{\bar{u}_{\lambda_2}(p_2)}{\sqrt{p_2^+}} \gamma^\mu \frac{u_{\lambda_1}(p_1)}{\sqrt{p_1^+}} \mathcal{R}_{\lambda_1 \lambda_2}^A \\ &= e \sum_j \mathcal{A}_j I_1(m_j, Q^2) [\epsilon_V^\mu (P_1 \cdot q) - P_1^\mu (\epsilon_V \cdot q)], \end{aligned} \quad (21)$$

where  $\mathbf{k}'_\perp = \mathbf{k}_\perp - x\mathbf{q}_\perp$ ,  $\mathcal{A}_j$  is the overlap of the  $j^{\text{th}}$  flavor portion of the flavor wavefunctions and contains all of the relevant charge factors and mixing amplitudes. Comparing the last line of Eq. (21) with Eq. (18) it can be seen that we have defined the form factor in terms of the charge and mixing amplitude independent quantity  $I_1(m_j, Q^2)$ .

The sum of the light-front spinors over the helicities in Eq. (21) is obtained as

$$\begin{aligned}
S^\mu &= \sum_{\lambda' s} \mathcal{R}_{\lambda_2 \bar{\lambda}}^{X^\dagger} \frac{\bar{u}_{\lambda_2}(p_2)}{\sqrt{p_2^+}} \gamma^\mu \frac{u_{\lambda_1}(p_1)}{\sqrt{p_1^+}} \mathcal{R}_{\lambda_1 \bar{\lambda}}^A \\
&= \frac{\text{Tr}[(\not{p}_{\bar{q}} - m_j) \Gamma_X (\not{p}_2 + m_j) \gamma^\mu (\not{p}_1 + m_j) \Gamma_A]}{\sqrt{p_1^+ p_2^+}}.
\end{aligned} \tag{22}$$

The explicit form of the trace is summarized in the Appendix. For  $V(P_1) \rightarrow S(P_2) \gamma^*(q)$  decay, the (transverse) polarization vector  $\epsilon_V$  of the vector meson is given by  $\epsilon_V(\pm) = [0, 0, \epsilon_\perp(\pm)]$  and the trace term with the plus component of the current is given by

$$S_{V \rightarrow S}^+ = \frac{-1}{(1-x)M_0 \sqrt{2}} \left\{ m_j [q^R - 4(1-x)k^R] - \frac{2k^R}{x(M_0 + 2m_j)} [(2x-1)^2 m_j^2 + \mathbf{k}_\perp^2 - x \mathbf{k}_\perp \cdot \mathbf{q}_\perp] \right\}, \tag{23}$$

where we use  $\epsilon_V(+)$ . Therefore, we obtain the one-loop integral,  $I_1(m_j, Q^2)$ , as follows

$$\begin{aligned}
I_1(m_j, Q^2) &= \int_0^1 dx \int \frac{d^2 \mathbf{k}_\perp}{16\pi^3} \phi_S(x, \mathbf{k}'_\perp) \phi_V(x, \mathbf{k}_\perp) \frac{1}{x(1-x)M_0} \left\{ x m_j [1 - 4(1-x) \frac{k^R q^L}{\mathbf{q}_\perp^2}] \right. \\
&\quad \left. - \frac{2(k^R q^L)/\mathbf{q}_\perp^2}{(M_0 + 2m_j)} [(2x-1)^2 m_j^2 + \mathbf{k}_\perp^2 - x \mathbf{k}_\perp \cdot \mathbf{q}_\perp] + (x \rightarrow 1-x, \mathbf{k}_\perp \rightarrow -\mathbf{k}_\perp) \right\},
\end{aligned} \tag{24}$$

where  $k^R q^L = \mathbf{k}_\perp \cdot \mathbf{q}_\perp - i|\mathbf{k}_\perp \times \mathbf{q}_\perp|_z$  and even though the cross term does not contribute to the integral, the dot product term does contribute.

Then, the transition form factor  $F_{VS\gamma^*}(Q^2)$  is given by

$$F_{VS\gamma^*}(Q^2) = \mathcal{A}_n I_1(m_n, Q^2) + \mathcal{A}_s I_1(m_s, Q^2), \tag{25}$$

where  $\mathcal{A}_n$  and  $\mathcal{A}_s$  are the overlaps of the up-down and strange portions of the flavor wavefunctions respectively.

For example, in the case where  $V = \phi$  and  $S = (u\bar{u} - d\bar{d})/\sqrt{2}$ ,  $\mathcal{A}_n = -(\sin \delta_{\omega-\phi})(e_u - e_d)/2$  and  $\mathcal{A}_s = 0$ . Also, for  $V = \phi$  and  $S = s\bar{s}$ ,  $\mathcal{A}_n = 0$  and  $\mathcal{A}_s = -(\cos \delta_{\omega-\phi})e_s$ .

The transition form factor  $F_{SV\gamma^*}(Q^2)$  for  $S(P_1) \rightarrow V(P_2) \gamma^*(q)$  can be obtained from Eq. (24) by replacing  $\mathbf{q}_\perp \rightarrow -\mathbf{q}_\perp$  and  $\mathbf{k}_\perp \rightarrow \mathbf{k}'_\perp$  and the explicit form for the one-loop integral corresponding to Eq. (24) is given by

$$\begin{aligned}
I'_1(m_j, Q^2) &= \int_0^1 dx \int \frac{d^2 \mathbf{k}_\perp}{16\pi^3} \phi_V(x, \mathbf{k}'_\perp) \phi_S(x, \mathbf{k}_\perp) \frac{1}{x(1-x)M'_0} \left\{ x m_j [-(2x-1)^2 - 4(1-x) \frac{k^R q^L}{\mathbf{q}_\perp^2}] \right. \\
&\quad \left. - \frac{2(k^R q^L - x \mathbf{q}_\perp^2)/\mathbf{q}_\perp^2}{(M'_0 + 2m_j)} [(2x-1)^2 m_j^2 + \mathbf{k}_\perp^2 - x \mathbf{k}_\perp \cdot \mathbf{q}_\perp] + (x \rightarrow 1-x; \mathbf{k} \rightarrow -\mathbf{k}_\perp) \right\},
\end{aligned} \tag{26}$$

where  $M_0'^2 = (m_j^2 + \mathbf{k}'_\perp^2)/x(1-x)$  and again the cross term in  $k^R q^L$  does not contribute to the integral. As one may expect, however, we found that  $I'_1(m_j, Q^2) = -I_1(m_j, Q^2)$  and thus  $F_{SV\gamma^*}(Q^2) = -F_{VS\gamma^*}(Q^2)$ .

## B. The process $S \rightarrow \gamma\gamma$

We now apply this model calculation to the two photon decays of scalar mesons. In this case, the coupling constant  $g_{S\gamma\gamma}$  for  $S \rightarrow \gamma\gamma$  is defined by

$$\begin{aligned}
\mathcal{M}_2 &= \langle \gamma(P_2) | \epsilon_1 \cdot J | S(P_1) \rangle \\
&= e^2 g_{S\gamma\gamma} [(\epsilon_1 \cdot \epsilon_2)(P_1 \cdot q) - (\epsilon_1 \cdot P_1)(\epsilon_2 \cdot q)],
\end{aligned} \tag{27}$$

where  $\epsilon_1 = \epsilon_\gamma(q)$  and  $\epsilon_2 = \epsilon_\gamma(P_2)$ . In terms of  $g_{S\gamma\gamma}$ , the decay width for this process is given by

$$\Gamma = \frac{\pi}{4} \alpha^2 g_{S\gamma\gamma}^2 M_S^3. \tag{28}$$

Here again, instead of calculating the two real photon decays, we first calculate the matrix element for  $S \rightarrow \gamma\gamma^*$ ,

which is given by

$$\begin{aligned}\mathcal{M}_2^\mu &= \langle \gamma(P_2) | J^\mu | S(P_1) \rangle, \\ &= e^2 F_{S\gamma\gamma^*}(Q^2) [\epsilon_2^\mu (P_1 \cdot q) - P_1^\mu (\epsilon_2 \cdot q)],\end{aligned}\quad (29)$$

and take the limit  $Q^2 \rightarrow 0$  to compute the decay rate for the two real photon decays. Using the same quark momentum variables in  $q^+ = 0$  frame as Eq. (20) with the plus component of the current, we then obtain

---


$$\begin{aligned}\mathcal{M}_2^+ &= \sqrt{n_c} \sum_j \mathcal{A}_j \sum_{\lambda_1, \lambda_2, \bar{\lambda}} \int_0^1 dx \int \frac{d^2 \mathbf{k}_\perp}{16\pi^3} \phi_S(x_i, \mathbf{k}_\perp) \left[ \frac{\bar{v}_{\bar{\lambda}}(p_{\bar{q}})}{\sqrt{p_{\bar{q}}^+}} \not{\epsilon}_2 \frac{u_{\lambda_2}(p_2)}{\sqrt{p_2^+}} \frac{\bar{u}_{\lambda_2}(p_2)}{\sqrt{p_2^+}} \gamma^+ \frac{u_{\lambda_1}(p_1)}{\sqrt{p_1^+}} \right. \\ &\quad \times \left. \frac{1}{\mathbf{q}_{\perp}^2 - [\mathbf{p}_{2\perp}^2 + m_j^2]/p_2^+ - [\mathbf{p}_{\bar{q}\perp}^2 + m_j^2]/p_{\bar{q}}^+} + (x \rightarrow 1-x, \mathbf{k}_\perp \rightarrow -\mathbf{k}_\perp) \right] \mathcal{R}_{\lambda_1 \lambda_{\bar{q}}}^S \\ &= e^2 \left( \sum_j \mathcal{A}_j I_2(m_j, Q^2) \right) [\epsilon_2^\mu (P_1 \cdot q) - P_1^\mu (\epsilon_2 \cdot q)],\end{aligned}\quad (30)$$

where  $\mathcal{A}_j$  now contains factors of  $e_j^2$  due to the presence of two electromagnetic vertices. As in the case of Eq. (22), the sum of the light-front spinors over the helicities in the first term of Eq. (30) is obtained as

$$\begin{aligned}T^\mu &= \sum_{\lambda_1, \lambda_2, \bar{\lambda}} \frac{\bar{v}_{\bar{\lambda}}(p_{\bar{q}})}{\sqrt{p_{\bar{q}}^+}} \not{\epsilon}_2 \frac{u_{\lambda_2}(p_2)}{\sqrt{p_2^+}} \frac{\bar{u}_{\lambda_2}(p_2)}{\sqrt{p_2^+}} \gamma^+ \frac{u_{\lambda_1}(p_1)}{\sqrt{p_1^+}} \mathcal{R}_{\lambda_1 \lambda_{\bar{q}}}^S \\ &= \frac{\text{Tr}[(\not{p}_{\bar{q}} - m_j) \not{\epsilon}_2 (\not{p}_2 + m_j) \gamma^+ (\not{p}_1 + m_j)]}{2\sqrt{2p_{\bar{q}}^+(p_2^+)^2 p_1^+}} \\ &= \frac{4m_j [p_1^+ (p_{\bar{q}} \cdot \epsilon_2 - p_2 \cdot \epsilon_2) + p_2^+ (p_{\bar{q}} \cdot \epsilon_2 - p_1 \cdot \epsilon_2) + p_{\bar{q}}^+ (p_2 \cdot \epsilon_2 - p_1 \cdot \epsilon_2)]}{2\sqrt{2p_{\bar{q}}^+(p_2^+)^2 p_1^+}},\end{aligned}\quad (31)$$

where we have used the fact that  $\epsilon_2^\pm(\pm) = 0$ . Now, using  $\epsilon_2(+) = (0, \sqrt{2}q^R/P_1^+, \epsilon_\perp)$ , we finally obtain the one loop integral,

$$\begin{aligned}I_2(m_j, Q^2) &= -\sqrt{6} \int_0^1 dx \int \frac{d^2 \mathbf{k}_\perp}{16\pi^3} \phi_S(x, \mathbf{k}_\perp) \left\{ \frac{m_j [(2x-1)^2 + 4(1-x)(k^R q^L / \mathbf{q}_\perp^2)]}{(1-x)\sqrt{x(1-x)}} \frac{x(1-x)}{m_j^2 + (\mathbf{k}_\perp - x\mathbf{q}_\perp)^2} \right. \\ &\quad \left. + (x \rightarrow 1-x, \mathbf{k}_\perp \rightarrow -\mathbf{k}_\perp) \right\},\end{aligned}\quad (32)$$

and the transition form factor is given by

$$F_{S\gamma\gamma^*}(Q^2) = \mathcal{A}_n I_2(m_n, Q^2) + \mathcal{A}_s I_2(m_s, Q^2).\quad (33)$$

As an example of the coefficients  $\mathcal{A}_{n,s}$ , consider the case where  $S = f_0(1370)$ . Here,  $\mathcal{A}_n = c_3 [(e_u^2 + e_d^2)/\sqrt{2}]$  and  $\mathcal{A}_s = b_3 e_s^2$ , where  $c_3$  and  $b_3$  are the glueball-quarkonia mixing amplitudes of Eq. (12).

## V. NUMERICAL RESULTS

### A. Decays involving $f_0(1370)$ , $f_0(1500)$ , and $f_0(1710)$

The expressions for the one-loop integrals,  $I_1(m_j, Q^2)$  and  $I_2(m_j, Q^2)$ , are evaluated numerically and used in Eqs. (25) and (33) to compute the  $Q^2$ -dependent transition form factors for  $\gamma\gamma^*$ ,  $\phi\gamma^*$ , and  $\rho\gamma^*$  decays of the

scalar mesons. As an example, we give the results for the case of the heavy glueball (*i.e.*  $M_{n\bar{n}} < M_{s\bar{s}} < M_{gg}$ ). The transition form factors for the  $\gamma\gamma^*$  process are shown in Fig. 2, and those for the  $\phi\gamma^*$  and  $\rho\gamma^*$  processes are collectively shown in Fig. 3. In the case of the two photon decay, the form factor should fall off like  $1/Q^2$  due to an intermediate quark propagator which becomes highly off-shell at large  $Q^2$ . Figure 4 shows the behavior of  $Q^2 \times F_{f_0\gamma\gamma^*}(Q^2)$  for each scalar state. Each of the curves clearly shows a tendency to flatten out, demonstrating  $1/Q^2$  dependence in the form factors.

The decay constants for the real photon processes can be obtained from the form factors in the limit as  $Q^2 \rightarrow 0$  (*i.e.*  $g = F(Q^2 = 0)$ ). In this limit, the values of the

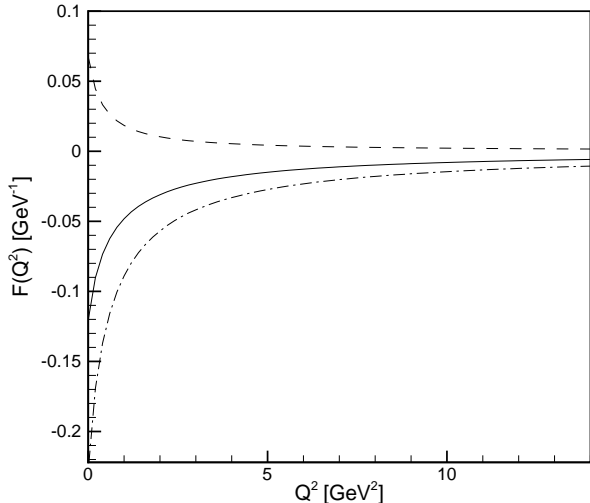


FIG. 2:  $f_0 \rightarrow \gamma\gamma^*$  transition form factors for  $f_0(1370)$  [dash-dotted],  $f_0(1500)$  [dashed], and  $f_0(1710)$  [solid].

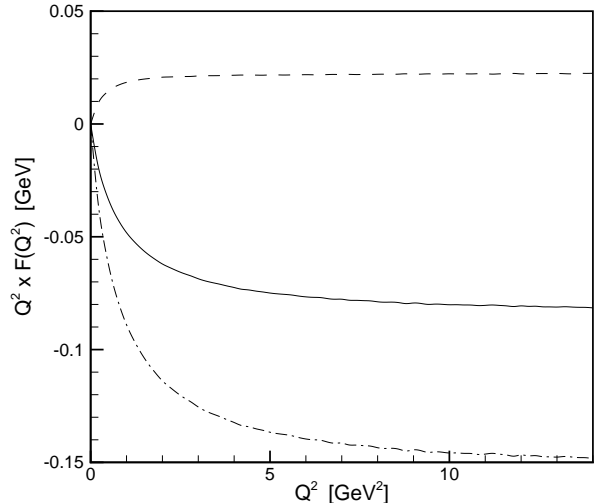


FIG. 4:  $Q^2$  times the  $f_0 \rightarrow \gamma\gamma^*$  transition form factors (Fig. 2) for  $f_0(1370)$  [dash-dotted],  $f_0(1500)$  [dashed], and  $f_0(1710)$  [solid].

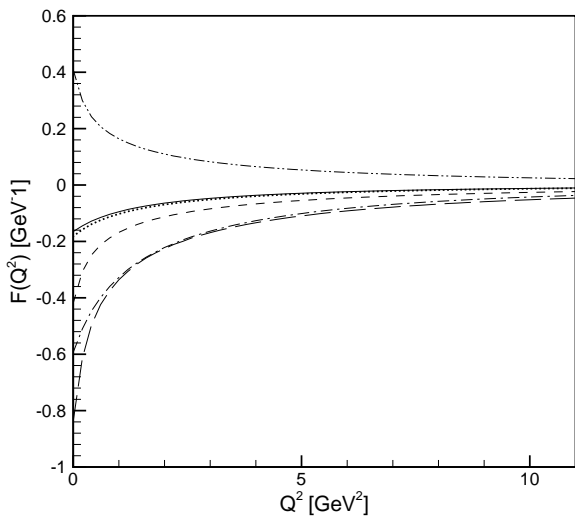


FIG. 3:  $f_0 \rightarrow \rho\gamma^*$  transition form factors for  $f_0(1370)$  [long-dashed],  $f_0(1500)$  [dash-dot-dotted], and  $f_0(1710)$  [short-dashed];  $f_0 \rightarrow \phi\gamma^*$  transition form factors for  $f_0(1370)$  [solid],  $f_0(1500)$  [dash-dotted], and  $f_0(1710)$  [dotted]. Here we have used  $\delta_{\omega-\phi} = +7.8^\circ$ .

one-loop integrals are

$$\begin{aligned}
 I_1(m_n, Q^2 = 0) &= 2.05 \text{ GeV}^{-1} \\
 I_1(m_s, Q^2 = 0) &= 1.93 \text{ GeV}^{-1} \\
 I_2(m_n, Q^2 = 0) &= -0.672 \text{ GeV}^{-1} \\
 I_2(m_s, Q^2 = 0) &= -0.375 \text{ GeV}^{-1}.
 \end{aligned} \tag{34}$$

The decay constants are obtained by substituting these

values into Eqs. (25) and (33). The decay widths are then calculated using Eqs. (17) and (28). The widths for the  $\gamma\gamma$ ,  $\phi\gamma$ , and  $\rho\gamma$  decays for all of the glueball mass scenarios are summarized in Tables I, II, and III respectively. The uncertainties in these values result solely from the uncertainties in the mixing amplitudes in Eqs. (13) and (14). We have not accounted for the uncertainties in the meson masses. The uncertainties in the masses of  $f_0(1500)$  and  $f_0(1710)$  ( $\sim 0.4\%$ ) are very small compared to the uncertainties in the mixing amplitudes (6%–40%), and can be neglected. However, the uncertainty in the mass of  $f_0(1370)$  is about 10%, and would, therefore, contribute significantly to the uncertainties in the decay widths.

Experimental data for radiative decays of the isoscalars  $f_0(1370)$ ,  $f_0(1500)$ , and  $f_0(1710)$  are poor. As one example, in the recent past the PDG had reported partial widths of  $3.8 \pm 1.5 \text{ keV}$  and  $5.4 \pm 2.3 \text{ keV}$  for the process  $f_0(1370) \rightarrow \gamma\gamma$  [24]. The PDG currently attributes these two values to  $f_0(600)$ , but at the same time they state in a footnote that this data could equally well be assigned to  $f_0(1370)$  [1]. If these data which are on the order of a few keV do belong to  $f_0(1370)$ , this would be encouraging given that our results listed in Table I are consistent with this order of magnitude. However, the ambiguity noted above makes any such comparison irrelevant, and a great deal more experimental investigation is necessary before any definitive conclusions can be reached about the validity of any of the glueball mixing schemes.

In the absence of good experimental data with which to compare our results, we turn to other theoretical predictions concerning these decay processes. In Ref. [18], Close and Kirk give predictions for ratios of  $f_0 \rightarrow \gamma\gamma$  widths

TABLE I: Decay widths for the process  $f_0 \rightarrow \gamma\gamma$ . The unit of the decay width is [keV]. The uncertainties result from the uncertainties in the mixing amplitudes in Eqs. (13) and (14).

	Light	Medium	Heavy
$f_0(1370)$	1.6	$3.9^{+0.8}_{-0.7}$	$5.6^{+1.4}_{-1.3}$
$f_0(1500)$	8.0	$4.1^{+1.0}_{-0.9}$	$0.65^{+0.72}_{-0.45}$
$f_0(1710)$	0.92	$1.3^{+0.2}_{-0.2}$	$3.0^{+1.4}_{-1.2}$

which depend only on charge factors and mixing amplitudes, and ignore all mass-dependent effects. For the ratios  $\Gamma(f_0(1710) \rightarrow \gamma\gamma) : \Gamma(f_0(1500) \rightarrow \gamma\gamma) : \Gamma(f_0(1370) \rightarrow \gamma\gamma)$  they obtain

$$\begin{aligned}
\text{Light Glueball} &= 1 : 5.1 : 2.8 \\
\text{Medium Glueball} &= 1 : 2.4 : 3.6 \\
\text{Heavy Glueball} &= 1 : 0.1 : 3.7 .
\end{aligned} \tag{35}$$

Our analysis which includes all of the relevant mass dependent effects yields

$$\begin{aligned}
\text{Light Glueball} &= 1 : 8.7 : 1.7 \\
\text{Medium Glueball} &= 1 : 3.2 : 3.0 \\
\text{Heavy Glueball} &= 1 : 0.2 : 1.9 .
\end{aligned} \tag{36}$$

Our results differ slightly from those of Close and Kirk, however the same overall qualitative pattern is preserved.

In Ref. [25], Close, Donnachie, and Kalashnikova (CDK) compute the  $\phi$  and  $\rho$  radiative decay widths for  $f_0(1370)$ ,  $f_0(1500)$ , and  $f_0(1710)$  in the NR quark model. Assuming that  $\phi = s\bar{s}$ , they obtain the values listed in Tables IV and V. Comparing these values with Tables II and III, it is clear that the relativistic corrections introduced by our model reduce the overall magnitudes of the decay widths by about 50–70%. We note somewhat greater reduction for the process of  $f_0(1370) \rightarrow \phi\gamma$  due to our non-zero  $\delta_{\omega-\phi}$ . A reduction in the widths would be expected given that the relativistic motion of the constituents tends to spread out the meson's wavefunction, thereby decreasing its peak value. Despite the differences in the overall magnitudes, however, the relative strengths between the different decay processes are fairly well preserved. Just as in CDK's analysis, we find that the largest branching ratio is likely to be that of  $f_0(1500) \rightarrow \rho\gamma$ . In our model, this branching ratio is about 1% for the light glueball case, 0.6% for the medium glueball case, and 0.2% for the heavy glueball case.

### B. Decays involving $a_0(980)$ and $f_0(980)$

If we assume  $a_0(980)$  to be a conventional  $q\bar{q}$ , then the flavor structure should be  $(u\bar{u} - d\bar{d})/\sqrt{2}$ . For the processes  $a_0(980) \rightarrow \gamma\gamma$  and  $\phi \rightarrow a_0(980)\gamma$ , the decay

TABLE II: Decay widths for the process  $f_0 \rightarrow \phi\gamma$ . The unit of the decay width is [keV]. These values are for  $\delta_{\omega-\phi} = +7.8^\circ$ . Using  $\delta_{\omega-\phi} = -7.8^\circ$  does not significantly alter the results. The uncertainties result from the uncertainties in the mixing amplitudes in Eqs. (13) and (14).

	Light	Medium	Heavy
$f_0(1370)$	0.98	$0.83^{+0.27}_{-0.23}$	$4.5^{+4.5}_{-3.0}$
$f_0(1500)$	7.5	$28^{+7}_{-6}$	$170^{+20}_{-20}$
$f_0(1710)$	450	$400^{+20}_{-20}$	$36^{+17}_{-14}$

TABLE III: Decay widths for the process  $f_0 \rightarrow \rho\gamma$ . The unit of the decay width is [keV]. The uncertainties result from the uncertainties in the mixing amplitudes in Eqs. (13) and (14).

	Light	Medium	Heavy
$f_0(1370)$	150	$390^{+80}_{-70}$	$530^{+120}_{-110}$
$f_0(1500)$	1100	$630^{+130}_{-120}$	$210^{+130}_{-100}$
$f_0(1710)$	24	$55^{+16}_{-14}$	$410^{+200}_{-160}$

constants and associated widths are calculated to be

$$\begin{aligned}
g_{\phi a_0\gamma} &= -0.14 \text{ GeV}^{-1}, & \Gamma_{\phi a_0\gamma} &= 2.8 \text{ eV} \\
g_{a_0\gamma\gamma} &= -0.16 \text{ GeV}^{-1}, & \Gamma_{a_0\gamma\gamma} &= 990 \text{ eV} .
\end{aligned} \tag{37}$$

Our result for the magnitude of  $g_{\phi a_0\gamma}$  is consistent with the theoretical calculations of Gokalp and Yilmaz [26], who obtain  $0.11 \pm 0.03 \text{ GeV}^{-1}$  using light-cone QCD sum rules, and Titov *et al.* [27], who obtain  $-0.16 \text{ GeV}^{-1}$  from phenomenological considerations. However, none of these calculated values for the widths are consistent with experimental data. The  $\phi$  radiative width of 2.8 eV gives a branching ratio of  $BR(\phi \rightarrow a_0\gamma) = 6.7 \times 10^{-7}$  which is significantly smaller than the PDG average of  $0.88^{+0.17}_{-0.17} \times 10^{-4}$ ; and, the two-photon width of 990 eV is roughly 3 times larger than the value reported by Amsler of  $0.30 \pm 0.10 \text{ keV}$  [28]. The flavor content of the isoscalar  $f_0(980)$  is less clear. If we consider the two possible extremes,  $f_0(980) = n\bar{n}$  and  $f_0(980) = s\bar{s}$ , we

TABLE IV: CDK's results for  $f_0 \rightarrow \phi\gamma$ . The unit of the decay width is [keV].

	Light	Medium	Heavy
$f_0(1370)$	8	9	32
$f_0(1500)$	9	60	454
$f_0(1710)$	800	718	78



TABLE V: CDK's results for  $f_0 \rightarrow \rho\gamma$ . The unit of the decay width is [keV].

	Light	Medium	Heavy
$f_0(1370)$	443	1121	1540
$f_0(1500)$	2519	1458	476
$f_0(1710)$	42	94	705

obtain

$$\begin{aligned}
 n\bar{n} &= \begin{cases} g_{\phi f_0\gamma} = -0.05 \text{ GeV}^{-1}, & \Gamma_{\phi f_0\gamma} = 0.37 \text{ eV} \\ g_{f_0\gamma\gamma} = -0.26 \text{ GeV}^{-1}, & \Gamma_{f_0\gamma\gamma} = 2.7 \text{ keV} \end{cases} \\
 s\bar{s} &= \begin{cases} g_{\phi f_0\gamma} = +0.64 \text{ GeV}^{-1}, & \Gamma_{\phi f_0\gamma} = 60 \text{ eV} \\ g_{f_0\gamma\gamma} = -0.04 \text{ GeV}^{-1}, & \Gamma_{f_0\gamma\gamma} = 63 \text{ eV}. \end{cases} \quad (38)
 \end{aligned}$$

The PDG average for the two photon width is  $\Gamma_{f_0\gamma\gamma} = 0.39_{-0.13}^{+0.10} \text{ keV}$ . Since the  $s\bar{s}$  result falls below this value and the  $n\bar{n}$  result sits above it, it would be possible for some mixed  $n\bar{n}$ - $s\bar{s}$  state to reproduce the data. Working out the mixing required for this, we find that  $f_0(980)$  would be about 6%  $n\bar{n}$  and 94%  $s\bar{s}$ . This alone would allow for  $f_0(980)$  to be interpreted as a conventional  $q\bar{q}$ . However, the  $\phi$  radiative widths we calculated lead to the branching ratios  $BR(\phi \rightarrow f_0\gamma) = 8.7 \times 10^{-8}$  for the  $n\bar{n}$  and  $BR(\phi \rightarrow f_0\gamma) = 1.4 \times 10^{-5}$  for the  $s\bar{s}$ . Both of these values fall well below the PDG average of  $3.3_{-0.5}^{+0.8} \times 10^{-4}$ . Also, if we compute the ratio  $BR(\phi \rightarrow f_0\gamma)/BR(\phi \rightarrow a_0\gamma)$  for our model predictions, we get 0.13 for  $f_0 = n\bar{n}$  and 21 for  $f_0 = s\bar{s}$ , while the experimental ratio is around 4. This again hints at the possibility of a mixed  $n\bar{n}$ - $s\bar{s}$  being able to reproduce the data. However, the mixing needed to reproduce this ratio requires that  $f_0(980)$  be 87%  $n\bar{n}$  and 13%  $s\bar{s}$ . This is the exact opposite of the mixing needed to reproduce the two photon width above. Overall our results are clearly inconsistent with the current experimental data on  $a_0(980)$  and  $f_0(980)$ . Therefore, we conclude that these states are most likely not  $q\bar{q}$ .

## VI. SUMMARY AND OUTLOOK

We have performed the first LFQM calculations involving scalar mesons. First, the  ${}^3P_0$  light-front wavefunction was constructed. It was shown that, in general, the covariant operator used to obtain the spin-orbit wavefunction depends explicitly on the relative momentum between the meson's constituents, and is, therefore, more complicated than the naive form that is commonly used. This wavefunction was used to compute radiative decays involving  $f_0(1370)$ ,  $f_0(1500)$ ,  $f_0(1710)$ ,  $f_0(980)$ , and  $a_0(980)$ . In the case of the three heavy isoscalars, the effects of glueball- $q\bar{q}$  mixing were taken into account. Specifically, three different mixing schemes corresponding to a heavy, medium, and light glueball were used.

The lack of good experimental data made it difficult to draw any conclusions about which of the three mixing scenarios, if any, could be the correct one. We note, however, that we have improved upon the earlier NR model predictions of Close *et al.* [25]. Relativistic corrections introduced by the LFQM resulted in decay widths that were about 50–70% smaller than those obtained in the NR calculations. Yet, very little change was observed in the pattern of relative strengths which is apparently quite robust. For the calculations involving  $a_0(980)$  and  $f_0(980)$ , we assumed these states to be  $q\bar{q}$ . In contrast to the case of the heavy scalars, there does exist well-established data for these light scalars. While one or two of the properties we calculated, when taken in isolation, could be considered consistent with the data, it is clear that our results as a whole do not match the data. This lends further support to the current idea that  $f_0(980)$  and  $a_0(980)$  are not  $q\bar{q}$  states.

In a future work, we intend to refine our analysis and perform our own glueball- $q\bar{q}$  mixing calculation using the LFQM. In this current work, the model parameters ( $m$ ,  $\beta$ ) used for the scalar ( ${}^3P_0$ ) meson wavefunction were obtained from a spectrum calculation fit to S-wave ( ${}^1S_0$  and  ${}^3S_1$ ) meson data. In order to improve the scalar wavefunction, we will perform a separate spectrum analysis using a QCD-inspired model Hamiltonian similar to that of Ref. [14], and fit the spectrum to P-wave ( ${}^3P_0$ ,  ${}^3P_1$ ,  ${}^3P_2$ , and  ${}^1P_1$ ) meson data. In addition to refining the model parameters, this analysis will also give the masses of the bare  $n\bar{n}$  and  $s\bar{s}$  P-wave quarkonia. With these masses, we will be able to perform a glueball- $q\bar{q}$  mixing analysis involving the isoscalars  $f_0(1370)$ ,  $f_0(1500)$ , and  $f_0(1710)$ . These mixing amplitudes, obtained using the LFQM, could then be compared with those of Lee-Weingarten and Close-Kirk.

## APPENDIX A: SPINOR STRUCTURE FOR $V(S) \rightarrow S(V)\gamma^*$ TRANSITION

In this appendix, we show the explicit form of the trace given by Eq. (22). For the  $V \rightarrow S\gamma^*$  transition, the following two trace calculations are necessary

$$\begin{aligned}
 S_{VS1}^+ &= \text{Tr}[(\not{p}_{\bar{q}} - m)(\not{p}_2 + m)\gamma^+(\not{p}_1 + m)\not{\epsilon}] \\
 &= 4m[p_1^+(\epsilon \cdot p_{\bar{q}} - \epsilon \cdot p_2) + p_2^+(\epsilon \cdot p_{\bar{q}} - \epsilon \cdot p_1) \\
 &\quad + p_{\bar{q}}^+(\epsilon \cdot p_1 - \epsilon \cdot p_2) \\
 &\quad + \epsilon^+(p_1 \cdot p_2 + p_2 \cdot p_{\bar{q}} - p_1 \cdot p_{\bar{q}} - m^2)], \\
 S_{VS2}^+ &= \text{Tr}[(\not{p}_{\bar{q}} - m)(\not{p}_2 + m)\gamma^+(\not{p}_1 + m)] \\
 &= 4[p_1^+(p_2 \cdot p_{\bar{q}} - m^2) + p_2^+(p_1 \cdot p_{\bar{q}} - m^2) \\
 &\quad + p_{\bar{q}}^+(m^2 - p_1 \cdot p_2)], \quad (A1)
 \end{aligned}$$

to get

$$S_{V \rightarrow S}^+ = \frac{-1}{4(1-x)M_0} \left[ S_{VS1}^+ - \frac{\epsilon \cdot (p_1 - p_{\bar{q}})}{M_0 + 2m} S_{VS2}^+ \right], \quad (A2)$$

where  $\epsilon = \epsilon(P_1)$  and we used the transverse polarizations in the calculation of the form factor and decay width.

On the other hand, for the  $S \rightarrow V\gamma^*$  transitions, we have

$$\begin{aligned}
S_{SV_1}^+ &= \text{Tr}[(\not{p}_{\bar{q}} - m) \not{\epsilon}' (\not{p}_2 + m) \gamma^+ (\not{p}_1 + m)] \\
&= 4m[p_1^+(\epsilon' \cdot p_{\bar{q}} - \epsilon' \cdot p_2) + p_2^+(\epsilon' \cdot p_{\bar{q}} - \epsilon' \cdot p_1) \\
&\quad - p_{\bar{q}}^+(\epsilon' \cdot p_1 - \epsilon' \cdot p_2) \\
&\quad + \epsilon'^+(p_1 \cdot p_2 + p_1 \cdot p_{\bar{q}} - p_2 \cdot p_{\bar{q}} - m^2)], \\
S_{SV_2}^+ &= \text{Tr}[(\not{p}_{\bar{q}} - m)(\not{p}_2 + m) \gamma^+ (\not{p}_1 + m)] \\
&= 4[p_1^+(p_2 \cdot p_{\bar{q}} - m^2) + p_2^+(p_1 \cdot p_{\bar{q}} - m^2) \\
&\quad + p_{\bar{q}}^+(m^2 - p_1 \cdot p_2)], \tag{A3}
\end{aligned}$$

to get

$$S_{S \rightarrow V}^+ = \frac{-1}{4(1-x)M_0'} \left[ S_{SV_1}^+ - \frac{\epsilon' \cdot (p_2 - p_{\bar{q}})}{M_0' + 2m} S_{SV_2}^+ \right], \tag{A4}$$

where  $\epsilon' = \epsilon'(P_2)$  and again we used the transverse polarizations in the calculation of the form factor and decay width.

## ACKNOWLEDGMENTS

MD would like to acknowledge the support from the SURA/Jlab fellowship. This work was supported in part by a grant from the U.S. Department of Energy (DE-FG02-96ER 40947) and the National Science Foundation (INT-9906384) and Kyungpook National University Research Fund, 2003. The North Carolina Supercomputing Center and the National Energy Research Scientific Computer Center are also acknowledged for the computing time.

- 
- [1] K. Hagiwara *et al.*, Phys. Rev. D **66**, 010001 (2002).
  - [2] J. Weinstein and N. Isgur, Phys. Rev. Lett. **48**, 659 (1982); Phys. Rev. D **41**, 2236 (1990).
  - [3] S. Godfrey and N. Isgur, Phys. Rev. D **32**, 189 (1985); R. Kokoski and N. Isgur, Phys. Rev. D **35**, 907 (1987).
  - [4] F. E. Barnes, Phys. Lett. B **165**, 434 (1985).
  - [5] C. Amsler and F. E. Close, Phys. Rev. D **53**, 295 (1996).
  - [6] V. V. Anisovich and A. V. Sarantsev, Phys. Lett. B **382**, 429 (1996).
  - [7] R. L. Jaffe, Phys. Rev. D **15**, 267 (1977); Phys. Rev. D **15**, 281 (1977); Phys. Rev. D **17**, 1444 (1978); R. L. Jaffe and K. Johnson, Phys. Lett. B **60**, 201 (1976).
  - [8] F.E. Close, N. Isgur, and S. Kumano, Nucl. Phys. B **389**, 513 (1993).
  - [9] N.A. Törnqvist and Matts Roos, Phys. Rev. Lett. **76**, 1575 (1996); N.A. Törnqvist, Z. Phys. C **68**, 647(1995).
  - [10] UKQCD Collaboration, G.Bali *et al.*, Phys. Lett. B **309**, 378 (1993).
  - [11] D. Weingarten, Nucl. Phys. B(Proc.Suppl.) **34**, 29(1994).
  - [12] F. E. Close and N. A. Törnqvist, hep-ph/0204205.
  - [13] S. Nussinv and T. N. Truong, Phys. Rev. Lett. **63**, 1349 (1989); Phys. Rev. Lett. **63**, 2003 (1989).
  - [14] H.-M. Choi and C.-R. Ji, Phys. Rev. D **59**, 074015 (1999)
  - [15] C.-R. Ji and H.-M. Choi, Heavy Ion Phys. **4**, 369 (1996); Few Body Syst. Suppl. **10**, 131 (1999); H.-M. Choi and C.-R. Ji, Phys. Rev. D **59**, 034001 (1999); Phys. Lett. B **460**, 461 (1999).
  - [16] Wolfgang Jaus, Phys. Rev. D **53**, 1349 (1996).
  - [17] W. Lee and D. Weingarten, Phys. Rev. D **61**, 014015 (1999).
  - [18] F. E. Close and A. Kirk, Eur. Phys. J. **C21**, 531 (2001).
  - [19] W.Jaus, Phys. Rev. D **41**, 3394 (1990); Phys. Rev. D **44**, 2851 (1991).
  - [20] P. L. Chung, F. Coester and W. N. Polyzou, Phys. Lett. B **205**, 545 (1988).
  - [21] C.-R. Ji, P. L. Chung, and S. R. Cotanch, Phys. Rev. D **45**, 4214 (1992).
  - [22] H.-M. Choi and C.-R. Ji, Nucl. Phys. A **618**, 291 (1997)
  - [23] G. P. Lepage and S. J. Brodsky, Phys. Rev. D **22**, 2157 (1980).
  - [24] D. E. Groom, *et al.*, Eur. Phys. J. **C15**, 1 (2000).
  - [25] F.E. Close, A. Donnachie, and Yu. S. Kalashnikova, hep-ph/0210293.
  - [26] A. Gokalp and O. Yilmaz, Phys. Lett. B **525**, 273 (2002).
  - [27] A. I. Titov, T.-S. H. Lee, H. Toki, and O. Streltsova, Phys. Rev. C **60**, 035205 (1999).
  - [28] C. Amsler, Rev. Mod. Phys. **70**, 1293 (1998).